Potentiometric, geometrical structure and molecular docking of some ligands and their metal complexes

M.A. Diab[1], A.Z. El-Sonbati[1], I.M. El-Deen[2], A.M. Mossalam[1]*

Abstract— Three organic ligands of 3-allyl-5-((4-derivative phenyl)diazenyl)-2-thioxothiazolidin-4-one (HL_n) were synthesized. The ligands (HL_n) were characterized showing a good agreement with those yielded from elemental analysis, IR and ^{1}H-NMR spectroscopy. The geometrical molecular structures of the ligands were optimized theoretically by HF method with 3-21G basis set and the quantum chemical parameters were explored by using molecular orbital calculations. Proton–ligand dissociation constants for HL_n ligands and their metal stability constants with Mn^{2+}, Co^{2+}, Ni^{2+} and Cu^{2+} in monomeric and polymeric forms were determined potentiometrically. The effect of temperature was discussed in detail showing a significant effect and the corresponding thermodynamic parameters (ΔG, ΔH and ΔS) were obtained. An attempt has been made with molecular docking to investigate and predict the binding between azo compounds with the receptor of prostate cancer 2q7k-Hormone and 3hb5-oxidoreductase receptor of breast cancer to provide a brief insight to the inhibition applicability. Finally, the dissociation process is non-spontaneous, endothermic and entropically unfavorable. The formation of the metal complexes has been found to be spontaneous, endothermic and entropically favorable. The presence of the azo group is an efficient inhibitor for prostate cancer 2q7k-Hormone and 3hb5-oxidoreductase receptor of breast cancer.

Keywords — Molecular docking, Molecular structure, Potentiometry, Thermodynamics

1. INTRODUCTION

The polymeric metal complexes [1,2] with coordination ligands have attracted considerable interests, because they gather the advantage of inorganic metal ions and conjugation polymer and have many advantages compared with inorganic and organic/aliphatic small molecule complexes. The polymeric metal complexes play an important role in many fields such as industrial chemistry [3], environmental studies [4], as well as medicinal [5] and analytical chemistry.

In the last years, the potentiometric titration technique of some organic compounds and their metal complexes in monomeric and polymeric forms has been extensively investigated through the determination of dissociation and stability constants, both from an experimental and a theoretical point of view [6,7]. One of the most striking features and implicit assumption of potentiometric technique is the measurement of the metal complex equilibrium in monomeric and polymeric forms to determine the average number of ligands coordinated with metal ion.

In continuation of our interest in studying behavior of dissociation and stability constants of some organic compounds and their metal complexes by potentiometric techniques [8-13], we synthesize and characterize some N-allyl rhodamine azo compounds and their metal complexes in monomeric and polymeric forms using spectroscopic techniques.

- [1]*Chemistry Department, Faculty of Science, Damietta University, Damietta 34517, Egypt*
- [2]*Chemistry Department, Faculty of Science, Port Said University, Port Said, Egypt*
- **Corresponding author: E-mail: ah.moslem@yahoo.com (A.M. Mossalam).*

Furthermore we report here the proton-ligand dissociation constants of N-allyl rhodamine and its metal stability constants with (Mn^{2+}, Co^{2+}, Ni^{2+} and Cu^{2+}) in monomeric and polymeric forms. On the other hand, a number of empirical relations of thermodynamic parameters (ΔG, ΔH and ΔS) have been derived and discussed.

Furthermore, some details have been overlooked when fitting experimental data to theoretical curves during the calculation of molecular docking that was used to predict the binding between azo compounds with the receptor of prostate cancer 2q7k-Hormone and 3hb5-oxidoreductase receptor of breast cancer. The molecular structure of the investigated ligands (HL_n) set are studied and quantum chemical parameters are calculated. The geometrical structures of the ligand are carried out by HF method with 3-21G basis set.

2. EXPERIMENTAL

2.1. Reagents and Materials

All the compounds and solvents used were purchased from Aldrich or Sigma and used as received without further purification. N- allylrhodanine was used without further purification. 2,2'-Azobisisobutyronitrile (AIBN) was used as initiator for all polymerizations. It was purified by dissolving it in hot ethanol and left to cool. The pure material was being collected by filtration and then dried [14].

2.2. Synthesis of allyl rhodanine azodyes

The organic compounds 3-allyl-5-((4-derivative phenyl)diazenyl)-2-thioxothiazolidin-4-one (HL_n) (Fig. 1) are prepared by gradual addition of an aqueous solution of 0.01 mol of sodium nitrite to a concentrated hydrochloric acid solu-

tion of 0.01 mol of *p*-aniline derivatives with stirring and kept for about 20 min. in an ice bath [15-17]. The formed diazonium chloride solutions were added gradually with vigorous stirring to a 0.01 mol cold solution of 3-allyl-4-hydroxythiazole-2(3H)-thione in 20 ml pyridine. The reaction mixture was stirred until coupling was complete. The solid precipitate was filtered, washed with water, dried and crystallized from ethanol and then dried in a vacuum desiccator over anhydrous calcium chloride.

2.3. Potentiometeric studies

2.3.1. Preparation of solutions

Ligands solution of 3-allyl-5-((4-derivative phenyl)diazenyl)-2-thioxothiazolidin-4-one (HL_n) (0.001 M) was prepared by dissolving an accurate weight of the solid in DMF (AnalaR). Metal ion solutions (0.0001 M) were prepared from AnalaR metal chlorides in bidistilled water and standardized with EDTA [14]. Solutions of 0.001 M (HCl) and 1 M (KCl) were also prepared in bidistilled water. A carbonate-free sodium hydroxide solution in a 50 % (by volume) DMF-water mixture was used as titrant and standardized against oxalic acid (AnalaR).

2.3.2. Apparatus and procedures for the potentiometric titrations

The apparatus model, general conditions and methods of calculation were the same as in previous work [18-21] based on alkaline potentiometric titrations. The following solution mixtures containing specific volumes (i)-(iii) were prepared and thoroughly mixed under continuous stirring.

i) 5 cm^3 0.001 M (HCl) + 5 cm^3 1 M (KCl) + 25 cm^3 DMF.

ii) 5 cm^3 0.001 M (HCl) + 5 cm^3 1 M (KCl) + 20 cm^3 DMF + 5 cm^3 0.00l M ligand.

iii) 5 cm^3 0.001 M (HCl) + 5 cm^3 l M (KCl) + 20 cm^3 DMF + 5 cm^3 0.001 M ligand + 10 cm^3 0.0001 M metal chloride.

The simultaneous Potentiometric titration of prepared solution mixtures carried out at 298 K against standard 0.002 M (NaOH) in a 50% (by volume) DMF-water mixture. Under continuous stirring the volume of added NaOH and pH values of solution were recorded. The titration was carried out between pH 4.0 and 12.0.

For each solution mixture, the volume was made up to 50 cm^3 with bidistilled water before the titration. The Potentiometric titrations also were carried out in the presence of 5 ml of AIBN (0.001 M) as initiator for the polymerization step. These titrations were repeated for temperatures of 308 and 318 K between pH 4.0 and 12.0.

2.4. Measurments

IR spectra (KBr discs, 4000–400 cm^{-1}) by Jasco-4100 spectrophotometer. ^{1}H-NMR spectrum was obtained with a Joel FX90 Fourier transform spectrometer with DMSO-d_6 as a solvent.

The molecular structures of the investigated compound were optimized by HF method with 3-21G basis set. The molecules were built with the Perkin Elmer ChemBio Draw and optimized using Perkin Elmer ChemBio 3D software [22-25]. Quantum chemical parameters such as the highest occupied molecular orbital energy (E_{HOMO}), the lowest unoccupied molecular orbital energy (E_{LUMO}) and HOMO–LUMO energy gap (ΔE) for the investigated molecules are calculated. In this study simulates the actual docking process in which the ligand–protein interaction energies are calculated using a Docking Server [26]. The MMFF94 Force field was used for energy minimization of ligand molecule using Docking Server. Gasteiger partial charges were added to the ligand atoms. Nonpolar hydrogen atoms were merged, and rotatable bonds were defined. Docking calculations were carried out on ligands (HL_n) protein models. Essential hydrogen atoms, Kollman united atom type charges, and solvation parameters were added with the aid of AutoDock tools [27]. Affinity (grid) maps of 0.375 Å spacing were generated using the Autogrid program [28]. Auto Dock parameter set- and distance-dependent dielectric functions were used in the calculation of the van der Waals and the electrostatic terms, respectively.

3. Results and Discussion

3.1. Infrared spectra spectra

The infrared spectra of the free ligands show no characteristic absorption assignable to NH_2 function. This confirms the formation of the azo compounds. The infrared spectrum of ligand exhibit strong to medium broad bands in the frequency ~3325 cm^{-1}. These bands can be attributed to intramolecular hydrogen bonded –OH group [29]. Furthermore, ligand exhibit a strong band due to C=O [29]. The discussed infrared features beside the band appeared at 1615 cm^{-1} can guide to assume the presence of C=N structure through resonating phenomena.

3.2. ^{1}H-NMR spectra

The ^{1}H NMR spectrum of ligands (HL_n) show two singlets corresponding to phenolic –OH and –NH. The singlet at δ 12.8 ppm and δ 10.9 ppm represent –OH and –NH, respectively of the formation of intramolecular hydrogen bonding with azonitrogen. The ligand do not show any peak attributed to enolic–OH proton indicating that they exist in keto form. Upon addition of D_2O the intensities of both OH and NH protons significant decrease. Further, the CH signal vanish and a new NH signal appear i.e., change from azo to hydrazone form. This supports the assignment. The protons of the aromatic ring resonate downfield in the δ 7.3–8.4 ppm range.

The ^{1}H NMR spectrum of HL_n monomers showed the expected peaks and pattern of the vinyl group (CH_2=CH), δ 6.25 ppm (dd, J = 17, 11 Hz) for the vinyl CH proton and proton δ 5.12 ppm (AM part of AMX system dd, J = 17, 1 Hz) for the vinyl CH_2 protons, respectively. These peaks disappeared on polymerization while a triplet at δ 1.86 ppm (t, J = 7 Hz) and a doublet at 1.80 ppm (d, J = 7 Hz) appeared, indicating

that the polymerization of HL_n monomer occurs on the vinyl group [30]. It is worth noting that the rest of the proton spectrum of the monomer and polymer remain almost without change.

3.3. Molecular structure

Geometry optimization option was employed to obtain the most stable structure. The molecular structures of ligands 3-allyl-5-((4-derivative phenyl)diazenyl)-2-thioxothiazolidin-4-one (HL_n) were optimized by HF method with 3-21G basis set. The molecules were built with the Perkin Elmer ChemBioDraw and optimized using Perkin Elmer ChemBio3D software. The HOMO–LUMO energy gap, ΔE, which is an important stability index, is applied to develop theoretical models for explaining the structure and conformation barriers in many molecular systems. From Table 1, forms (B) of HL_n ligands have smaller ΔE values indicate that their structures are more stable than the forms (A) (Fig. 1). The calculated molecular structures of stable form B for HL_n are shown in Fig. 2. Also corresponding geometric parameters bond lengths and bond angles of HL_n are tabulated in Tables 2 and 3. In our present study, the corresponding bond lengths of C5-C6 and C5-O7 are calculated as 1.356 and 1.364 Å, these values are lesser than the rhodanine molecule due to the attachment of *p*-anline derivatives. On the other hand, the C-C bond length (C10-C11, C11-C12, C12-C13, C13-C14, C14-C15 and C15-C10) of six membered rings are relatively equal to 1.35 Å. The bond angles of N(4)-C(3)-S(2), N(4)-C(3)-S(8), S(2)-C(3)-S(8), C(3)-S(2)-C(6), C(6)-C(5)-N(4), N(4)-C(5)-O(7), C6-C5-O7 and H21-O7-C5 are equal 108, 130, 121, 94, 114, 123, 123 and 110, respectively. These bond angles are relatively equal to simple rhodanine molecule [31].

The HOMO and LUMO for form B of the ligands (HL_n) are shown in Fig. 3. According to the frontier molecular orbital theory, FMO, the chemical reactivity is a function of interaction between HOMO and LUMO levels of the reacting species [32]. The E_{HOMO} often associated with the electron donating ability of the molecule to donate electrons to appropriated acceptor molecules with low-energy, empty molecular orbital. Similarly, E_{LUMO} indicates the ability of the molecule to accept electrons. The lower value of E_{LUMO} indicates the high ability of the molecule is to accept electrons [33]. While, the higher is the value of E_{HOMO} of the inhibitor, the easer is its offering electrons. Stability of ligands increases with the order $HL_3 < HL_2 < HL_1$ related to ΔE values which are tabulated in Table 1, as expected from Hammett's constant (σ^R) (Fig. 4).

Additional parameters such as separation energies, ΔE, absolute electronegativities, χ, chemical potentials, Pi, absolute hardness, η, absolute softness, σ, global electrophilicity, ω, global softness, *S*, and additional electronic charge, ΔN_{max}, have been calculated according to the following equations (1-8) [34]:

$$\Delta E = E_{LUMO} - E_{HOMO} \quad (1)$$

$$\chi = \frac{-(E_{HOMO} + E_{LUMO})}{2} \quad (2)$$

$$\eta = \frac{E_{LUMO} - E_{HOMO}}{2} \quad (3)$$

$$\sigma = 1/\eta \quad (4)$$

$$Pi = -\chi \quad (5)$$

$$S = \frac{1}{2\eta} \quad (6)$$

$$\omega = Pi^2 / 2\eta \quad (7)$$

$$\Delta N_{max} = -Pi/\eta \quad (8)$$

3.4. Molecular docking

Molecular docking aims to achieve an optimized conformation for both the protein and drug with relative orientation between them such that the free energy of the overall system is minimized. Docking study showed the binding affinity, number of hydrogen bonds. It is interesting to note that the binding affinities have negative values. This reveals the high feasibility of this reaction. Molecular docking is a key tool in computer drug design [35,36].

In this context, the docked ligands were analysis with the prostate cancer mutant 2q7k-Hormone and breast cancer 3hb5 as shown in Fig. 5(A, C, E) and (B, D, F) and Fig. 6(A1, C1, E1) and (B1, D1, F1). The study simulates the actual docking process in which the ligand–protein pair-wise interaction energies are calculated in Tables 5 and 6. According to our results, HB plot curve indicates that, azo compound binds to the two proteins with hydrogen bond interactions of ligands (HL_n) with 2q7k and 3hb5 as shown in Figs. 7 and 8. The calculated efficiency is favorable, K_i values estimated by AutoDock were compared with experimental K_i values, when available, and the Gibbs free energy is negative [37,38]. Also, based on this data, we can propose that interaction between the 2q7k and 3hb5 receptors and the ligands (HL_n) is possible. 2D plot curve of docking with ligands (HL_n) is shown in Figs. 9 and 10.

This interaction could activate apoptosis in cancer cell energy of interactions with ligands (HL_n). From the analysis of the values, it is evident that the binding energy of ligands (HL_n) decreases. So that is decrease in binding energy of HL_n on transpiration of mutation for prostate cancer 2q7k whereas increase with HL_n for breast cancer. Binding energies are most widely used mode of measuring binding affinity of a ligand.
Thus, the decrease in binding energy due to mutation will increase the binding affinity of the allylrhodanine azodye derivatives towards the receptor. Their characteristic feature represents the presence of several active sites available for hydrogen bonding. This feature gives them the ability to be good binding inhibitors to the protein and will help to produce augmented inhibitory compounds. The results confirm that, the azo ligand derived from 3-allylrhodanine is an efficient inhibitor of prostate cancer.

Molecular docking and binding energy calculations of ligands (HL_n) with prostate cancer mutant 2q7k-hormone and breast cancer mutant 3hb5-oxidoreductase receptors indicated that the ligands (HL_n) are efficient inhibitors of 3hb5-oxidoreductase and 2q7k-hormone receptors.

3.4.1. Species distribution curves

Docking measurements can be used as a new technique for prediction of the dissociation constants, pK_a. From microspecies distribution curves obtained by docking measurements for the ligands, it was found that, there is one dissociable proton, pK^H, nearly in the range ~7.0-7.6 for ligands (HL_n) as shown in Fig. 11. The predicted K_i and experimently calculated pK^H values of the ligands.

3.5. Proton-ligand dissociation constant

The interaction of a metal with an electron donor atom of ligands (HL_n) is usually followed by the release of H^+. Alkaline potentiometric titrations are based on the detection of the protons released upon complexation in this direction it is possible to calculate the dissociation constants and the stability constants of its complexes from the potentiometric titration.

The acid dissociation constant of ligands (HL_n) was first determined from titration curves in the presence and absence of ligands (HL_n). It can be seen that for the same volume of NaOH added, the compound titration curves show a lower pH value than the titration curve of free acid. From these titration curves, the average number of protons associated with HL_n molecule, $\bar{n}_A$, in monomeric forms were determined at different pH values applying the following equation (9) according to Irving and Rossotti equation [39,40]

$$\bar{n}_A = Y \pm \frac{(V_1 - V_2)(N^o + E^o)}{(V^o - V_1)TC_L^o} \qquad (9)$$

where Y is the number of available protons in HL_n (Y=1) and V_1 and V_2 are the volumes of alkali required to reach the same pH on the titration curve of hydrochloric acid and reagent, respectively, V^o is the initial volume (50 cm^3) of the mixture, $TC°_L$ is the total concentration of the reagent, N° is the normality of the sodium hydroxide solution and E° is the initial concentration of the free acid. The average number of protons associated with the ligands (HL_n) at different pH values, $\bar{n}_A$ was calculated. Thus, the formation curves ($\bar{n}_A$ *vs.* pH) for the proton-ligand systems were constructed and found to extend between 0 and 1 in the $\bar{n}_A$ scale. This means that ligands (HL_n) has one dissociable proton (the hydrogen ion of the -OH rhodanine moiety, pK^H) are listed in Table 5. The PHL_n has a lower acidic character (higher pK^H values) than HL_n. This is quite reasonable because the presence of the vinyl group (H_2C=CH) in monomeric form will decrease the electron density, whereby weaker -OH bond is formed. The absence of vinyl group in polymeric form will lead to the opposite effect (i.e., retard the removal of the ligand proton and hence increase the basicity of ligands (HL_n).

3.6. Stability constants

Dissociation constant behavior and the effect of metal ion on the ligand titration curve provides a selective means for measuring stability constants of metal complexes by the same way potentiometrically. The formation curves for the metal complexes were obtained by plotting the average number of ligands attached per metal ions ($\bar{n}$) (calculated according to Irving and Rossotti [40,41]); versus the free ligand exponent (pL), can be calculated using the Eqs. 10 and 11.

$$\bar{n} = \frac{(V_3 - V_2)(N^o + E^o)}{(V^o - V_2).\bar{n}_A.TC_M^o} \qquad (10)$$

and

$$pL = \log_{10} \frac{\sum_{n=o}^{n=J} \beta_n^H \left(\frac{1}{[H^+]}\right)^n}{TC_L^o - \bar{n}.TC_M^o} . \frac{V^o + V_3}{V^o} \qquad (11)$$

where $TC°_M$ is the total concentration of the metal ion present in the solution, $\beta^H{}_n$ is the overall proton-reagent stability constant. V_1, V_2 and V_3 are the volumes of alkali required to reach the same pH on the titration curves of hydrochloric acid, organic ligand and complex, respectively. The values of the stability constants (log K_1 and log K_2) are given in Table 6.

The following general remarks can be made:

i) The maximum value of $\bar{n}$ was ~ 2 indicating the formation of 1:1 and 1:2 (metal:ligand) complexes [42].

ii) The metal ion solution used in the present study was very dilute (2 x 10^{-5} M), hence there was no possibility of formation of metal hydroxide and polynuclear complexes [43,44].

iii) The metal titration curves were displaced to the right-hand side of the ligand titration curves along the volume axis, indicating proton release upon complex formation of the metal ion with the ligand. The large decrease in pH for the metal titration curves relative to ligand titration curves point to the formation of strong metal complexes [45,46].

iv) For all the complexes, the stability constants of PHL_n are higher than HL_n. This is quite reasonable because the ligand in polymeric forms are better complexing agent [14].

v) For the same ligand (HL_n and PHL_n) at constant temperature, the stability of the chelates increases in the order Mn^{2+}, Co^{2+}, Ni^{2+}, Cu^{2+} [47-49]. This order largely reflects that the stability of Cu^{2+} complexes are considerably larger as compared to other metals of the 3d series. Under the influence of both the polarizing ability of the metal ion [50] and the ligand field [51], Cu^{2+} will receive some extra stabilization due to tetragonal distortion of octahedral symmetry in its complexes. The greater stability of Cu^{2+} complexes is produced by the well known *Jahn–Teller* ef-

fect [52].

3.7. Effect of temperature

The dissociation constants (pK^H), for ligands (HL_n) set in monomeric and polymeric forms as well as the stability constants of its complexes with (Mn^{2+}, Co^{2+}, Ni^{2+} and Cu^{2+}) have been evaluated at 298, 308 and 318 K which are listed in Tables 5 and 6.

The enthalpy change (ΔH°) for the dissociation or complexation process was calculated from the slope of the plot (pK^a or log K *vs.* 1/T) using the graphical representation of the van Hoff equation (12) or (13). *i.e.,* the complexation produces a sufficient change in the pK^a.

$$\Delta G^\circ = -2.303\, RT \log K = \Delta H^\circ - T\,\Delta S^\circ \quad (12)$$

or

$$\log K = \left(\frac{-\Delta H^o}{2.303R}\right)\left(\frac{1}{T}\right) + \frac{\Delta S^o}{2.303R} \quad (13)$$

From the ΔG° and ΔH° values one can deduce the ΔS using the well known relationships 12 and 14:

$$\Delta S^\circ = (\Delta H^\circ - \Delta G^\circ) / T \quad (14)$$

where R = 8.314 J K^{-1} mol^{-1} is the gas constant, K is the dissociation constant for the ligand or the stability constant of the complex, and T is absolute temperature.

All thermodynamic parameters of the dissociation process of ligands (HL_n) set in monomeric and polymeric forms are recorded in Tables 6,7 and 8. From these results the following conclusions can be made:

i) The pK^H values decrease with increasing temperature, *i.e.,* the acidity of the ligand increases.
ii) A positive value of ΔH indicates that the process is endothermic.
iii) A large positive value of ΔG° indicates that the dissociation process is not spontaneous [53].
iv) A negative value of ΔS° is obtained due to the increased order as a result of the solvation process.

All the thermodynamic parameters of the stepwise stability constants of ligands (HL_n) complexes set in monomeric and polymeric forms are recorded in Tables 5 and 7.

It is known that the divalent metal ions exist in solution as octahedrally hydrated species [54] and the obtained values of ΔH° and ΔS° can then be considered as the sum of two contributions: (a) release of H_2O molecules, and (b) metal-ligand bond formation. Examination of these values shows that:

i) The stepwise stability constants (log K_1 and log K_2) for HL_n and PHL_n complexes increases with increasing temperature [55].
ii) The negative value of ΔG° for the complexation process of HL_n and PHL_n suggests the spontaneous nature of such processes [56, 57].
iii) The ΔH° values of HL_n and PHL_n are positive, meaning that these processes are endothermic and favourable at higher temperature.
iv) The ΔS° values for the complexes of HL_n and PHL_n are positive, confirming that the complex formation is entropically favourable [14].

4. CONCLUSION

A series of three closely related organic ligand compounds consisting 3-allyl-5-((4-derivative phenyl)diazenyl)-2-thioxothiazolidin-4-one (HL_n) has been designed, synthesized and characterized by different spectroscopic techniques. Calculated geometries investigated to obtain the most stable structure. Simultaneous potentiometric titration analysis for the solution of ligands (HL_n) and its metal stability constants with (Mn^{2+}, Co^{2+}, Ni^{2+} and Cu^{2+}) in monomeric and polymeric forms was established with good prediction ability. The proton–ligand dissociation constant of ligands (HL_n) and metal–ligand stability constants of their complexes with metal ions (Mn^{2+}, Co^{2+}, Ni^{2+} and Cu^{2+}) at different temperatures were determined. At constant temperature the stability constants of the formed complexes decrease in the order of $Mn^{2+} > Co^{2+} > Ni^{2+} > Cu^{2+}$. From This performance, the dissociation process is non spontaneous, endothermic and entropically unfavorable. The formation of the metal complexes has been found to be spontaneous, endothermic and entropically favorable based on thermodynamic principles. The values of stability constants (log K_1 and log K_2) of complexes increase with increasing temperature. The molecular docking performance of these ligands (HL_n) set observed an indication that presence of azo group is an efficient inhibitor for prostate cancer 2q7k-Hormone and 3hb5-oxidoreductase receptor of breast cancer.

Table 1: E_{HOMO}, E_{LUMO} and some chemical parameters of HL_n

Comp.		E_{HOMO} (a.u)	E_{LUMO} (a.u)	ΔE (a.u)	χ (a.u)	η (a.u)	σ $(a.u)^{-1}$	Pi (a.u)	S $(a.u)^{-1}$	ω (a.u)	ΔN_{max}
HL_1	(A)	-3.336	-2.415	0.921	2.876	0.461	2.172	-2.875	1.085	8.977	6.24
	(B)	-2.303	-2.247	0.056	2.275	0.028	35.714	-2.275	17.857	92.422	81.250
HL_2	(A)	-3.363	-2.948	0.415	3.156	0.208	4.819	-3.156	2.409	23.993	15.21
	(B)	-2.433	-2.245	0.188	2.339	0.094	10.638	-2.339	5.319	29.101	24.88
HL_3	(A)	-3.330	-2.302	1.028	2.816	0.514	1.946	-2.816	0.973	7.714	5.48
	(B)	-2.244	-2.032	0.212	2.138	0.106	9.434	-2.138	4.717	21.56	20.17

Table 2: Bond lengths for ligands (HL_n).

Bond lengths(Å)					
HL_1		**HL_2**		**HL_3**	
C(19)-H(32)	1.1	C(18)-H(29)	1.1	C(19)-H(29)	1.1
C(19)-H(31)	1.101	C(18)-H(28)	1.101	C(19)-H(28)	1.101
C(18)-H(30)	1.104	C(17)-H(27)	1.104	C(18)-H(27)	1.104
C(17)-H(29)	1.114	C(16)-H(26)	1.114	C(17)-H(26)	1.114
C(17)-H(28)	1.113	C(16)-H(25)	1.113	C(17)-H(25)	1.113
C(16)-H(27)	1.114	C(15)-H(24)	1.103	C(15)-H(24)	1.103
C(16)-H(26)	1.114	C(14)-H(23)	1.103	C(14)-H(23)	1.103
C(16)-H(25)	1.113	C(12)-H(22)	1.105	C(12)-H(22)	1.105
C(15)-H(24)	1.103	C(11)-H(21)	1.103	C(11)-H(21)	1.103
C(14)-H(23)	1.103	C(10)-H(20)	1.103	O(7)-H(20)	0.972
C(12)-H(22)	1.105	O(7)-H(19)	0.972	C(10)-C(15)	1.342
C(11)-H(21)	1.103	C(10)-C(15)	1.341	C(14)-C(15)	1.343
O(7)-H(20)	0.972	C(14)-C(15)	1.343	C(13)-C(14)	1.348
C(10)-C(15)	1.344	C(13)-C(14)	1.348	C(12)-C(13)	1.348
C(14)-C(15)	1.343	C(12)-C(13)	1.348	C(11)-C(12)	1.342
C(13)-C(14)	1.347	C(11)-C(12)	1.342	C(10)-C(11)	1.341
C(12)-C(13)	1.347	C(10)-C(11)	1.341	C(3)-S(2)	1.79
C(11)-C(12)	1.342	C(3)-S(2)	1.79	C(6)-S(2)	1.486
C(10)-C(11)	1.343	C(6)-S(2)	1.486	C(5)-C(6)	1.356
C(3)-S(2)	1.79	C(5)-C(6)	1.356	N(4)-C(5)	1.274
C(6)-S(2)	1.486	N(4)-C(5)	1.274	C(3)-N(4)	1.265
C(5)-C(6)	1.356	C(3)-N(4)	1.265	C(18)-C(19)	1.34
N(4)-C(5)	1.274	C(17)-C(18)	1.34	C(17)-C(18)	1.507
C(3)-N(4)	1.265	C(16)-C(17)	1.508	N(4)-C(17)	1.479
C(18)-C(19)	1.34	N(4)-C(16)	1.479	C(13)-N(1)	1.269
C(17)-C(18)	1.508	C(13)-N(1)	1.269	C(10)-Cl(16)	1.727
N(4)-C(17)	1.479	C(6)-N(9)	1.268	C(6)-N(9)	1.268
C(13)-N(1)	1.268	N(1)-N(9)	1.252	N(1)-N(9)	1.252
C(10)-C(16)	1.51	C(3)-S(8)	1.573	C(3)-S(8)	1.573
C(6)-N(9)	1.268	C(5)-O(7)	1.364	C(5)-O(7)	1.364
N(1)-N(9)	1.252				
C(3)-S(8)	1.573				
C(5)-O(7)	1.364				

Table 3: Bond angles for ligands (HL_n).

Bond angles (°)					
HL_1		**HL_2**		**HL_3**	
H(32)-C(19)-H(31)	117.569	H(29)-C(18)-H(28)	117.562	H(29)-C(19)-H(28)	117.563
H(32)-C(19)-C(18)	121.407	H(29)-C(18)-C(17)	121.409	H(29)-C(19)-C(18)	121.407
H(31)-C(19)-C(18)	121.024	H(28)-C(18)-C(17)	121.029	H(28)-C(19)-C(18)	121.031
H(30)-C(18)-C(19)	119.064	H(27)-C(17)-C(18)	119.071	H(27)-C(18)-C(19)	119.072
H(30)-C(18)-C(17)	116.995	H(27)-C(17)-C(16)	116.998	H(27)-C(18)-C(17)	117
C(19)-C(18)-C(17)	123.941	C(18)-C(17)-C(16)	123.931	C(19)-C(18)-C(17)	123.928
H(27)-C(16)-H(26)	108.468	H(24)-C(15)-C(10)	119.647	H(24)-C(15)-C(10)	120.478
H(27)-C(16)-H(25)	107.795	H(24)-C(15)-C(14)	120.031	H(24)-C(15)-C(14)	119.321
H(27)-C(16)-C(10)	110.016	C(10)-C(15)-C(14)	120.322	C(10)-C(15)-C(14)	120.201
H(26)-C(16)-H(25)	107.196	H(20)-C(10)-C(15)	120.315	C(15)-C(10)-C(11)	119.499
H(26)-C(16)-C(10)	110.67	H(20)-C(10)-C(11)	120.287	C(15)-C(10)-Cl(16)	120.251
H(25)-C(16)-C(10)	112.55	C(15)-C(10)-C(11)	119.398	C(11)-C(10)-Cl(16)	120.25
H(24)-C(15)-C(10)	119.328	H(21)-C(11)-C(12)	120.119	H(21)-C(11)-C(12)	119.418
H(24)-C(15)-C(14)	119.408	H(21)-C(11)-C(10)	119.894	H(21)-C(11)-C(10)	120.726
C(10)-C(15)-C(14)	121.264	C(12)-C(11)-C(10)	119.987	C(12)-C(11)-C(10)	119.855
C(15)-C(10)-C(11)	117.927	H(23)-C(14)-C(15)	116.997	H(23)-C(14)-C(15)	116.994
C(15)-C(10)-C(16)	120.449	H(23)-C(14)-C(13)	121.933	H(23)-C(14)-C(13)	121.834
C(11)-C(10)-C(16)	121.624	C(15)-C(14)-C(13)	121.07	C(15)-C(14)-C(13)	121.172
H(21)-C(11)-C(12)	119.204	H(22)-C(12)-C(13)	120.365	H(22)-C(12)-C(13)	120.272
H(21)-C(11)-C(10)	119.959	H(22)-C(12)-C(11)	118.175	H(22)-C(12)-C(11)	118.155
C(12)-C(11)-C(10)	120.837	C(13)-C(12)-C(11)	121.46	C(13)-C(12)-C(11)	121.573
H(23)-C(14)-C(15)	117.075	H(26)-C(16)-H(25)	104.126	H(26)-C(17)-H(25)	104.122
H(23)-C(14)-C(13)	121.897	H(26)-C(16)-C(17)	108.426	H(26)-C(17)-C(18)	108.415
C(15)-C(14)-C(13)	121.028	H(26)-C(16)-N(4)	111.755	H(26)-C(17)-N(4)	111.766
H(22)-C(12)-C(13)	120.272	H(25)-C(16)-C(17)	111.401	H(25)-C(17)-C(18)	111.411
H(22)-C(12)-C(11)	118.232	H(25)-C(16)-N(4)	111.223	H(25)-C(17)-N(4)	111.211
C(13)-C(12)-C(11)	121.496	C(17)-C(16)-N(4)	109.779	C(18)-C(17)-N(4)	109.785
H(29)-C(17)-H(28)	104.113	S(2)-C(3)-N(4)	103.702	S(2)-C(3)-N(4)	103.699
H(29)-C(17)-C(18)	108.458	S(2)-C(3)-S(8)	124.816	S(2)-C(3)-S(8)	124.815
H(29)-C(17)-N(4)	111.733	N(4)-C(3)-S(8)	131.446	N(4)-C(3)-S(8)	131.451
H(28)-C(17)-C(18)	111.386	H(19)-O(7)-C(5)	110.182	H(20)-O(7)-C(5)	110.196
H(28)-C(17)-N(4)	111.255	C(5)-N(4)-C(3)	117.115	C(5)-N(4)-C(3)	117.126
C(18)-C(17)-N(4)	109.765	C(5)-N(4)-C(16)	120.83	C(5)-N(4)-C(17)	120.841
S(2)-C(3)-N(4)	103.704	C(3)-N(4)-C(16)	122.055	C(3)-N(4)-C(17)	122.033
S(2)-C(3)-S(8)	124.811	C(3)-S(2)-C(6)	93.879	C(3)-S(2)-C(6)	93.876
N(4)-C(3)-S(8)	131.447	C(6)-C(5)-N(4)	113.86	C(6)-C(5)-N(4)	113.846
H(20)-O(7)-C(5)	110.179	C(6)-C(5)-O(7)	123.147	C(6)-C(5)-O(7)	123.158
C(5)-N(4)-C(3)	117.113	N(4)-C(5)-O(7)	122.972	N(4)-C(5)-O(7)	122.975
C(5)-N(4)-C(17)	120.807	C(14)-C(13)-C(12)	117.763	C(14)-C(13)-C(12)	117.699
C(3)-N(4)-C(17)	122.08	C(14)-C(13)-N(1)	125.647	C(14)-C(13)-N(1)	125.692
C(3)-S(2)-C(6)	93.876	C(12)-C(13)-N(1)	116.589	C(12)-C(13)-N(1)	116.609
C(6)-C(5)-N(4)	113.857	S(2)-C(6)-C(5)	111.413	S(2)-C(6)-C(5)	111.423
C(6)-C(5)-O(7)	123.152	S(2)-C(6)-N(9)	131.465	S(2)-C(6)-N(9)	131.407
N(4)-C(5)-O(7)	122.969	C(5)-C(6)-N(9)	117.122	C(5)-C(6)-N(9)	117.169
C(14)-C(13)-C(12)	117.448	C(6)-N(9)-N(1)	119.3	C(6)-N(9)-N(1)	119.3
C(14)-C(13)-N(1)	125.777	C(13)-N(1)-N(9)	119.622	C(13)-N(1)-N(9)	119.648
C(12)-C(13)-N(1)	116.775				
S(2)-C(6)-C(5)	111.418				
S(2)-C(6)-N(9)	131.477				
C(5)-C(6)-N(9)	117.105				
C(6)-N(9)-N(1)	119.311				
C(13)-N(1)-N(9)	119.569				

Table 4. Energy values obtained in docking calculations of ligands (HL_n) with of prostate cancer mutant 2q7k and breast cancer mutant 3hb5 receptors.

Receptor		Est. free energy of binding (kcal/mol)	Est. inhibition constant (K_i) (μM)	vdW+ bond+ desolve energy (kcal/mol)	Electrostatic Energy (kcal/mol)	Total inter-cooled Energy (kcal/mol)	Interact surface
2q7k	HL_1	-6.65	13.28	-7.93	-0.00	-7.93	539.824
	HL_2	-7.09	6.34	-8.38	-0.01	8.39	511.396
	HL_3	-4.08	1.01	-6.07	-0.00	-6.07	540.873
3hb5	HL_1	-6.71	12.05	-8.11	+0.01	-8.10	778.469
	HL_2	-6.03	37.79	-7.73	+0.03	-7.70	751.366
	HL_3	-7.52	3.08	-8.83	-0.04	-8.87	765.084

Table 5: Thermodynamic functions for the dissociation of HL_{1-3} and PHL_{1-3} in 50 % (by volume) DMF-water mixture in the presence of 0.1 M KCl at different temperatures.

Comp.	Temp. K	Dissociation constant	Free energy change kJ mol^{-1}	Enthalpy change kJ mol^{-1}	Entropy change J mol^{-1} K^{-1}
		pK^H	ΔG	ΔH	$-\Delta S$
HL_1	298	8.31	47.42		70.89
	308	8.17	48.18	26.29	71.07
	318	8.02	48.83		70.89
HL_2	298	8.10	46.22		85.13
	308	7.99	47.12	20.85	85.29
	318	7.87	47.92		85.12
HL_3	298	7.90	45.08		66.12
	308	7.77	45.82	25.37	66.39
	318	7.62	46.40		66.11
PHL_1	298	8.82	50.33		86.74
	308	8.69	51.25	24.48	86.92
	318	8.55	52.06		86.74
PHL_2	298	8.61	49.13		91.75
	308	8.48	50.01	21.79	91.64
	318	8.37	50.96		91.75
PHL_3	298	8.41	47.99		78.76
	308	8.26	48.71	24.52	78.56
	318	8.14	49.56		78.76

Table 6: Stepwise stability constants for ML and ML_2 complexes of HL_{1-3} and PHL_{1-3} in 50 % (by volume) DMF-water mixture in the presence of 0.1 M KCl at different temperatures.

Comp.	M^{n+}	298 K		308 K		318 K	
		log K_1	log K_2	log K_1	log K_2	log K_1	log K_2
HL_1	Mn^{2+}	5.00	4.20	5.18	4.37	5.37	4.56
	Co^{2+}	5.18	4.37	5.35	4.53	5.47	4.71
	Ni^{2+}	5.24	4.43	5.41	4.58	5.52	4.75
	Cu^{2+}	5.44	4.61	5.62	4.79	5.70	4.90
HL_2	Mn^{2+}	5.15	4.34	5.32	4.55	5.85	4.74
	Co^{2+}	5.33	4.49	5.47	4.70	6.03	4.89
	Ni^{2+}	5.41	4.63	5.63	4.84	6.20	5.06
	Cu^{2+}	5.60	4.75	5.79	4.96	6.36	5.23
HL_3	Mn^{2+}	5.32	4.52	5.50	4.73	6.03	4.92
	Co^{2+}	5.46	4.66	5.64	4.88	6.19	5.05
	Ni^{2+}	5.61	4.81	5.80	5.01	6.33	5.20
	Cu^{2+}	5.76	4.95	5.95	5.17	6.46	5.36
PHL_1	Mn^{2+}	6.00	5.02	6.28	5.30	6.56	5.60
	Co^{2+}	6.14	5.15	6.43	5.44	6.71	5.75
	Ni^{2+}	6.29	5.29	6.56	5.58	6.85	5.91
	Cu^{2+}	6.43	5.44	6.70	5.72	6.99	6.04
PHL_2	Mn^{2+}	6.18	5.20	6.46	5.48	6.74	5.78
	Co^{2+}	6.31	5.33	6.61	5.61	6.90	5.91
	Ni^{2+}	6.46	5.48	6.76	5.76	7.03	6.05
	Cu^{2+}	6.61	5.62	6.90	5.91	7.16	6.19
PHL_3	Mn^{2+}	6.36	5.38	6.64	5.66	6.92	5.96
	Co^{2+}	6.48	5.51	6.79	5.80	7.07	6.11
	Ni^{2+}	6.63	5.65	6.92	5.93	7.21	6.26
	Cu^{2+}	6.77	5.79	7.06	6.06	7.35	6.40

Table 7: Thermodynamic functions for ML and ML_2 complexes of HL_{1-3} in 50 % (by volume) DMF-water mixture and 0.1 M KCl at different temperatures.

Comp.	M^{n+}	T/K	Free energy change (kJ mol^{-1})		Enthalpy change (kJ mol^{-1})		Entropy change (J mol^{-1} K^{-1})	
			$-\Delta G_1$	$-\Delta G_2$	ΔH_1	ΔH_2	ΔS_1	ΔS_2
HL_1	Mn^{2+}	298	28.53	23.96	33.55	32.63	208.31	189.91
		308	30.55	25.77	33.55	32.63	208.10	189.61
		318	32.70	27.76	33.55	32.63	208.31	189.92
	Co^{2+}	298	29.56	24.93	26.35	30.82	187.60	187.08
		308	31.55	26.71	26.35	30.82	187.99	186.79
		318	33.31	28.68	26.35	30.82	187.59	187.09
	Ni^{2+}	298	29.90	25.28	25.45	29.00	185.74	182.14
		308	31.90	27.01	25.45	29.00	186.22	181.85
		318	33.61	28.92	25.45	29.00	185.73	182.15
	Cu^{2+}	298	31.04	26.30	23.68	23.68	183.62	167.72
		308	33.14	28.25	23.68	23.68	184.48	168.59
		318	34.71	29.84	23.68	23.68	183.60	168.28
HL_2	Mn^{2+}	298	29.39	24.76	63.13	36.30	310.45	204.90
		308	31.37	26.83	63.13	36.30	306.83	204.96
		318	35.62	28.86	63.13	36.30	310.53	204.90

	Co^{2+}	298	30.41	25.62	63.07	36.30	313.70	207.77
		308	32.26	27.72	63.07	36.30	309.51	207.84
		318	36.72	29.77	63.07	36.30	313.79	207.77
	Ni^{2+}	298	30.87	26.42	71.30	38.99	342.86	219.48
		308	33.20	28.54	71.30	38.99	339.30	219.25
		318	37.75	30.81	71.30	38.99	342.93	219.49
	Cu^{2+}	298	31.95	27.10	68.55	43.47	337.26	236.83
		308	34.15	29.25	68.55	43.47	333.43	236.12
		318	38.72	31.84	68.55	43.47	337.35	236.85
HL_3	Mn^{2+}	298	30.36	25.79	64.05	36.30	316.79	208.34
		308	32.44	27.89	64.05	36.30	313.25	208.41
		318	36.72	29.96	64.05	36.30	316.86	208.34
	Co^{2+}	298	31.15	26.59	65.84	35.42	325.49	208.08
		308	33.26	28.78	65.84	35.42	321.76	208.43
		318	37.69	30.75	65.84	35.42	325.57	208.07
	Ni^{2+}	298	32.01	27.45	64.96	35.38	325.41	210.82
		308	34.20	29.55	64.96	35.38	321.97	210.79
		318	38.54	31.66	64.96	35.38	325.49	210.82
	Cu^{2+}	298	32.87	28.24	63.17	37.21	322.27	219.65
		308	35.09	30.49	63.17	37.21	319.02	219.81
		318	39.33	32.64	63.17	37.21	322.34	219.65

Table 8 : Thermodynamic functions for ML and ML_2 complexes of PHL_{1-3} in 50 % (by volume) DMF-water mixture and 0.1 M KCl at different temperatures.

Comp.	M^{n+}	T/K	Free energy change (kJ mol^{-1})		Enthalpy change (kJ mol^{-1})		Entropy change (J mol^{-1} K^{-1})	
			$-\Delta G_1$	$-\Delta G_2$	ΔH_1	ΔH_2	ΔS_1	ΔS_2
PHL_1	Mn^{2+}	298	34.24	28.64	50.79	52.58	285.31	272.57
		308	37.04	31.26	50.79	52.58	285.14	272.20
		318	39.94	34.10	50.79	52.58	285.31	272.57
	Co^{2+}	298	35.03	29.39	51.70	54.39	291.07	281.14
		308	37.92	32.08	51.70	54.39	290.99	280.77
		318	40.86	35.01	51.70	54.39	291.07	281.15
	Ni^{2+}	298	35.89	30.18	50.77	56.19	290.80	289.84
		308	38.69	32.91	50.77	56.19	290.43	289.27
		318	41.71	35.98	50.77	56.19	290.80	289.85
	Cu^{2+}	298	31.04	26.30	23.68	26.37	183.62	176.76
		308	33.14	28.25	23.68	26.37	184.48	177.33
		318	34.71	29.84	23.68	26.37	183.60	176.74
PHL_2	Mn^{2+}	298	35.26	29.67	50.79	52.58	288.76	276.01
		308	38.10	32.32	50.79	52.58	288.58	275.64
		318	41.04	35.19	50.79	52.58	288.76	276.02
	Co^{2+}	298	36.00	30.41	53.52	52.58	300.41	278.50
		308	38.98	33.08	53.52	52.58	300.32	278.13
		318	42.01	35.98	53.52	52.58	300.41	278.51
	Ni^{2+}	298	36.86	31.27	51.72	51.68	297.26	278.36
		308	39.87	33.97	51.72	51.68	297.37	278.09
		318	42.80	36.84	51.72	51.68	297.26	278.37
	Cu^{2+}	298	37.72	32.07	49.91	51.70	294.04	281.11
		308	40.69	34.85	49.91	51.70	294.16	281.03
		318	43.60	37.69	49.91	51.70	294.04	281.11
PHL_3	Mn^{2+}	298	36.29	30.70	50.79	52.58	292.20	279.46
		308	39.16	33.38	50.79	52.58	292.03	279.09

	318	42.13	36.29	50.79	52.58	292.21	279.47
Co^{2+}	298	36.97	31.44	53.54	54.39	303.73	288.03
	308	40.04	34.20	53.54	54.39	303.83	287.66
	318	43.05	37.20	53.54	54.39	303.73	288.04
Ni^{2+}	298	37.83	32.24	52.60	55.27	303.46	293.66
	308	40.81	34.97	52.60	55.27	303.28	293.00
	318	43.90	38.12	52.60	55.27	303.46	293.67
Cu^{2+}	298	38.63	33.04	52.60	55.25	306.14	296.27
	308	41.64	35.74	52.60	55.25	305.96	295.42
	318	44.75	38.97	52.60	55.25	306.14	296.29

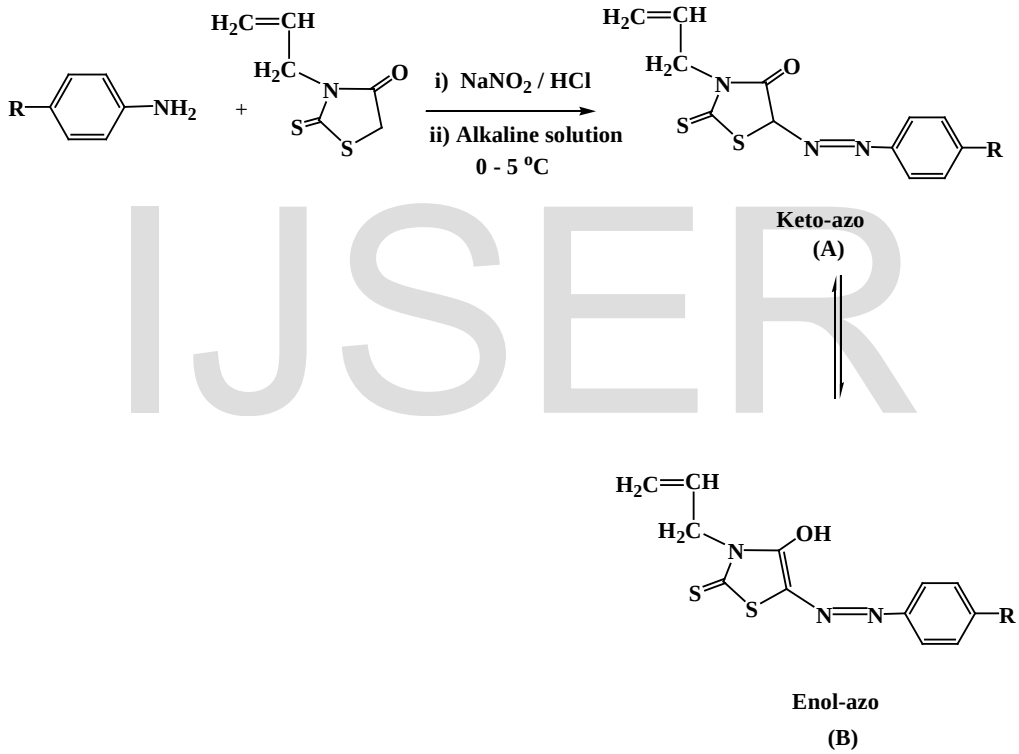

Fig. 1: The formation mechanism of allylrhodanine azodye (HL_n); (where R = $-CH_3$ (HL_1), -H (HL_2) and –Cl (HL_3)) in monomeric form.

HL_1

HL_2

HL_3

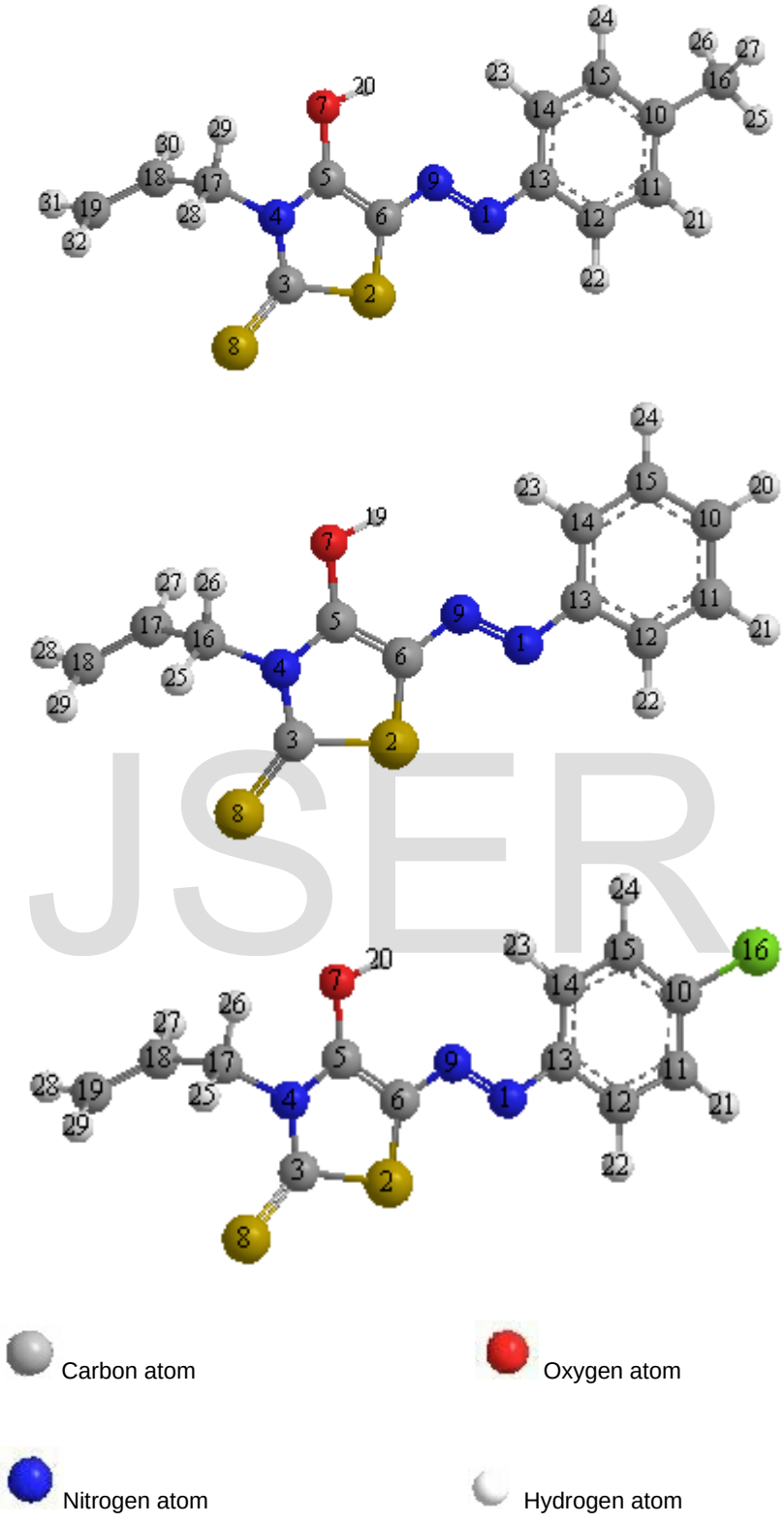

Fig. 2: Molecular structure with atomic numbering of HL_n in monomeric form.

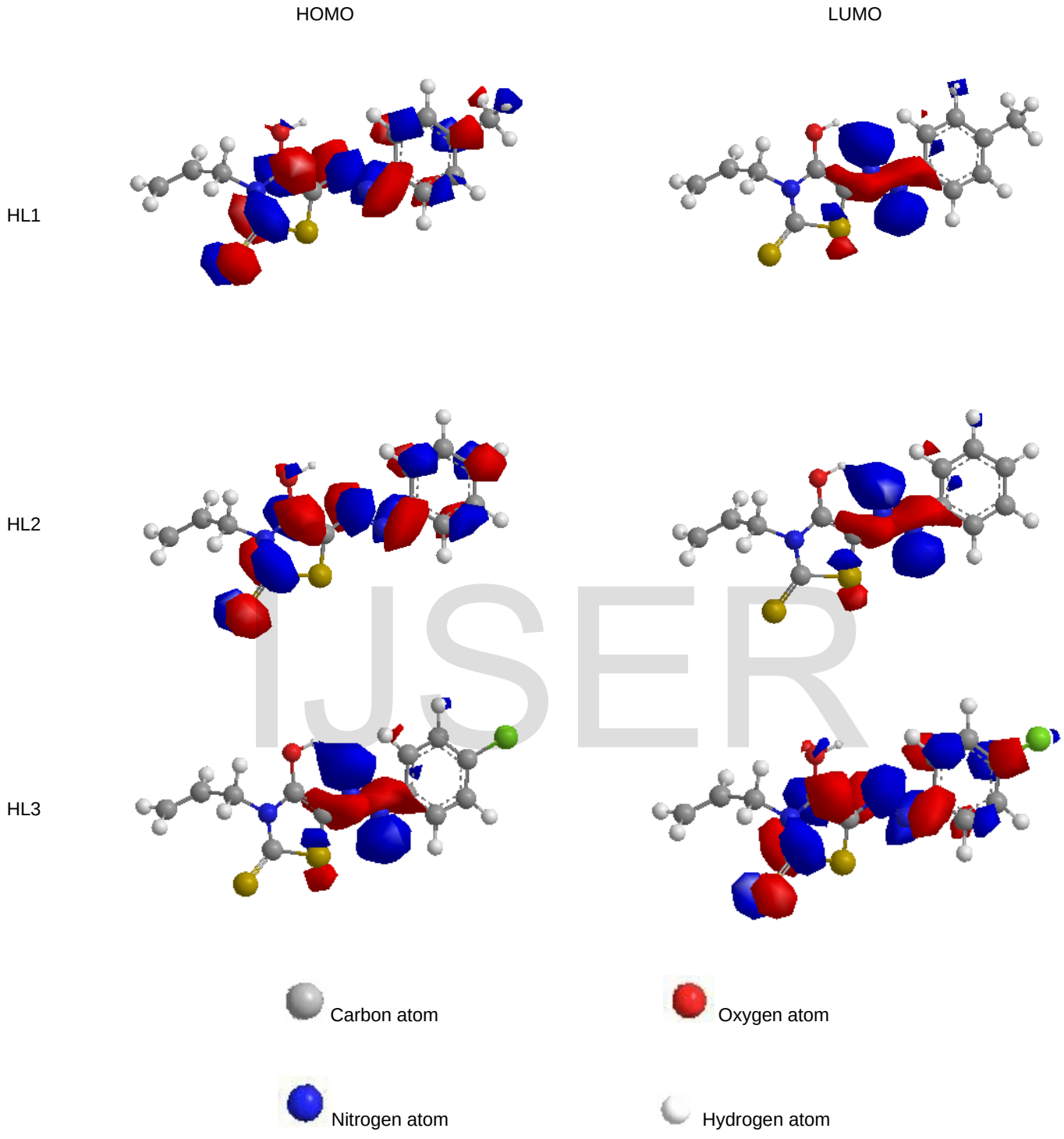

Fig. 3: Molecular structures (HOMO & LUMO) for HL_n ligands.

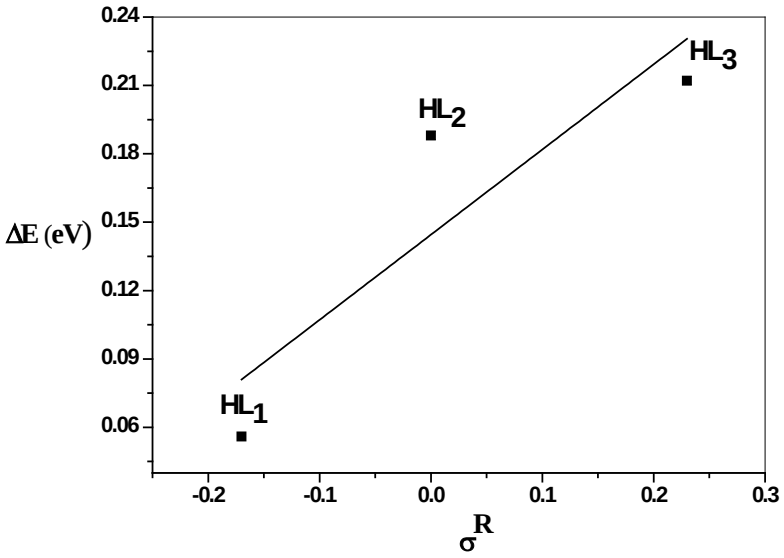

Fig. 4: The relation between Hammett's substitution coefficients (σ^R) *vs.* energy gap (ΔE) of the ligands ($\mathbf{HL_n}$).

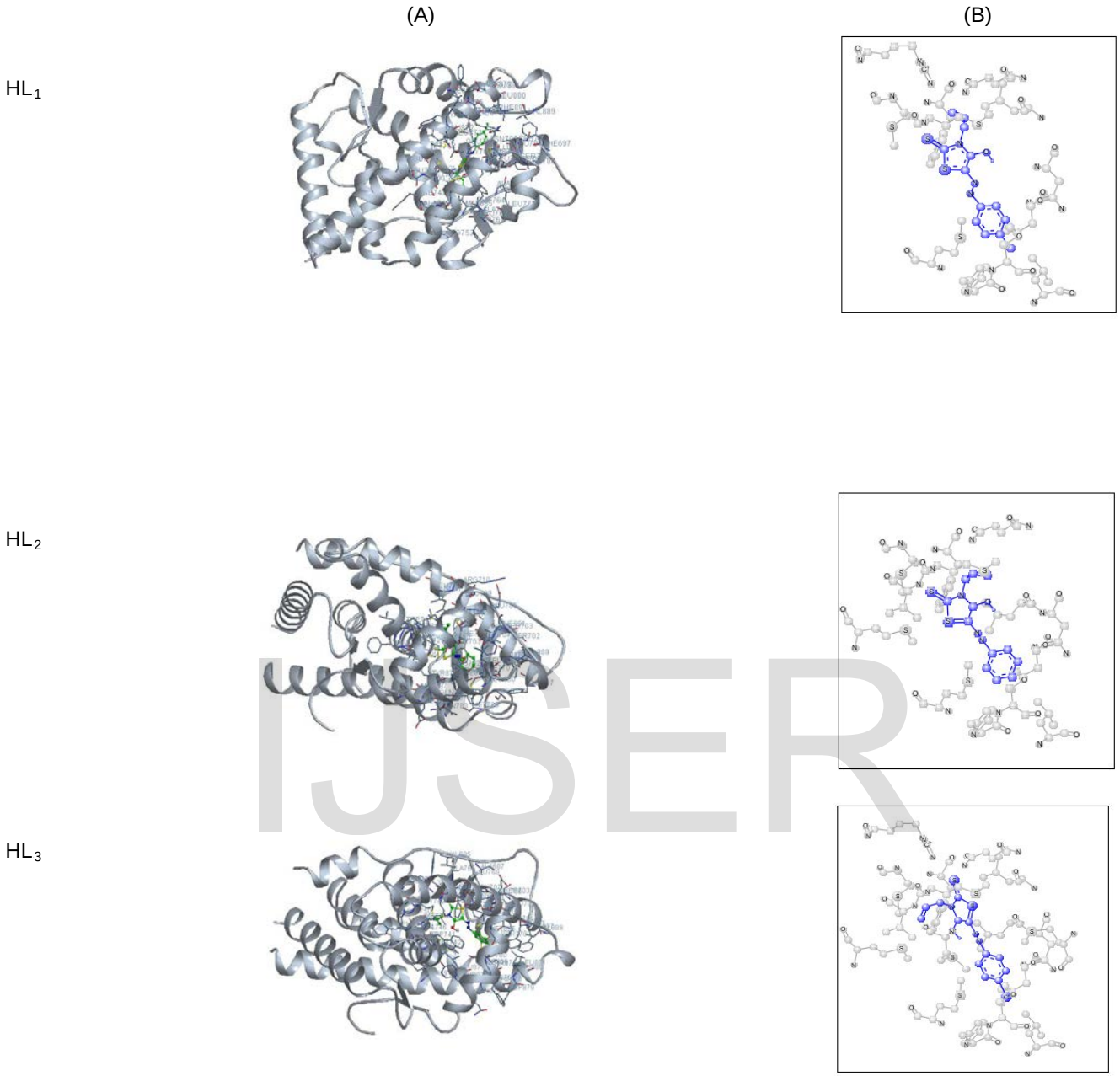

Fig. 5. The ligands (HLn) (green in (A) and blue in (B)) in interaction with prostate cancer mutant 2q7k receptor. (For interpretation of the references to color in this figure legend, the reader is referred to the web version of this article).

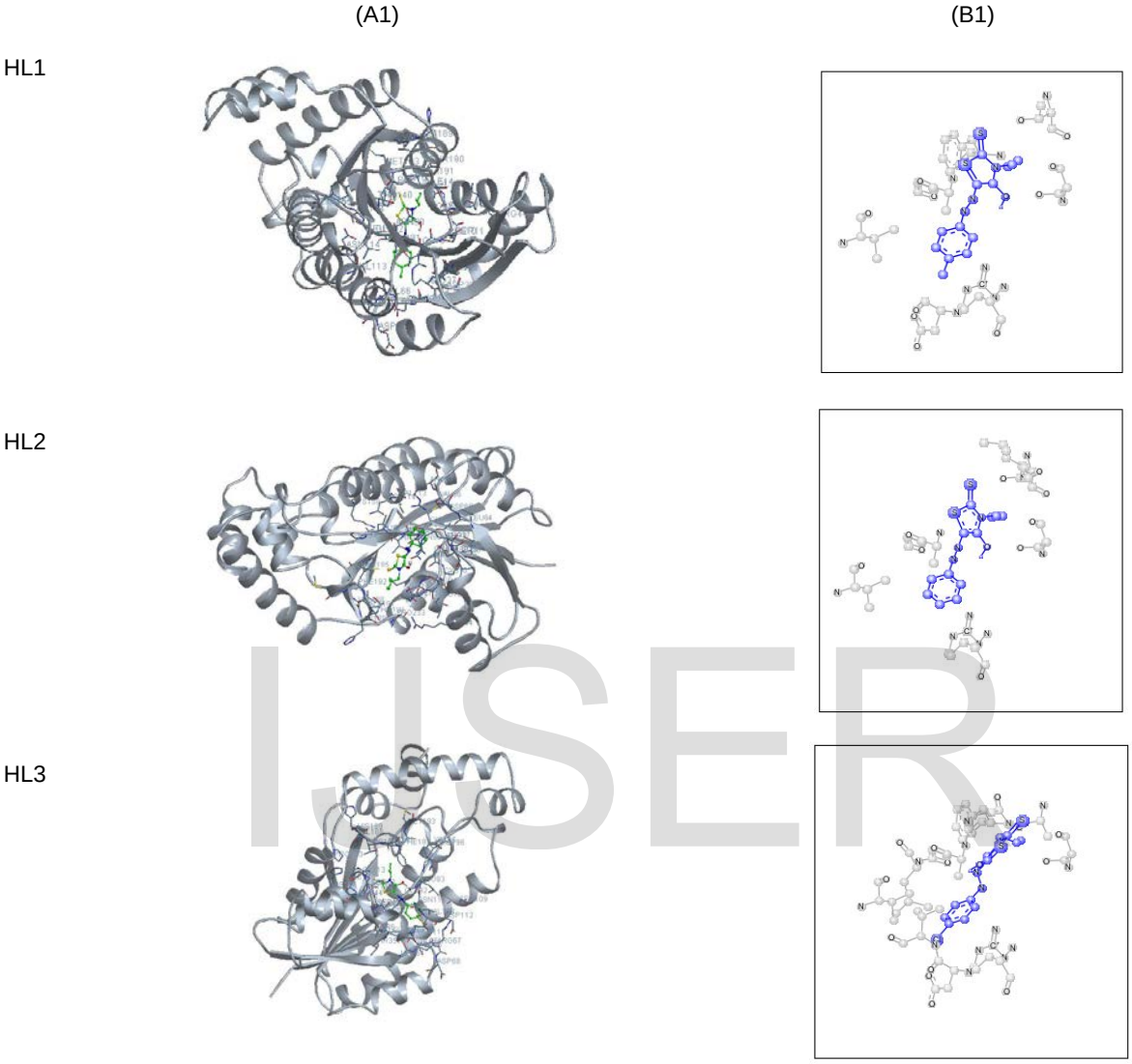

Fig. 6. The ligands (HLn) (green in (A1) and blue in (B1)) in interaction with breast cancer mutant 3hb5 receptor. (For interpretation of the references to color in this figure legend, the reader is referred to the web version of this article).

HL1

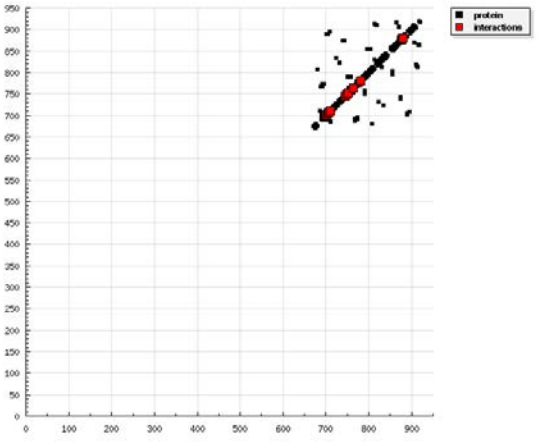

HL2

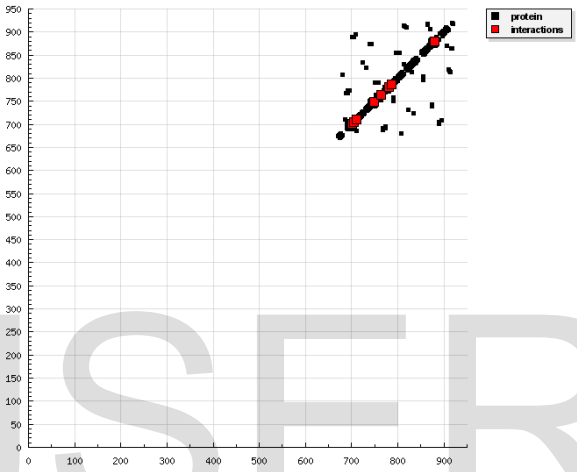

HL3

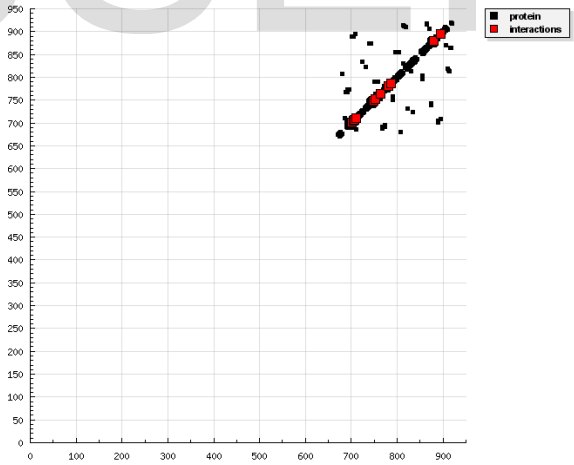

Fig. 7. HB plot of interaction between ligands (HL_n) with receptor of prostate cancer mutant 2q7k.

HL1

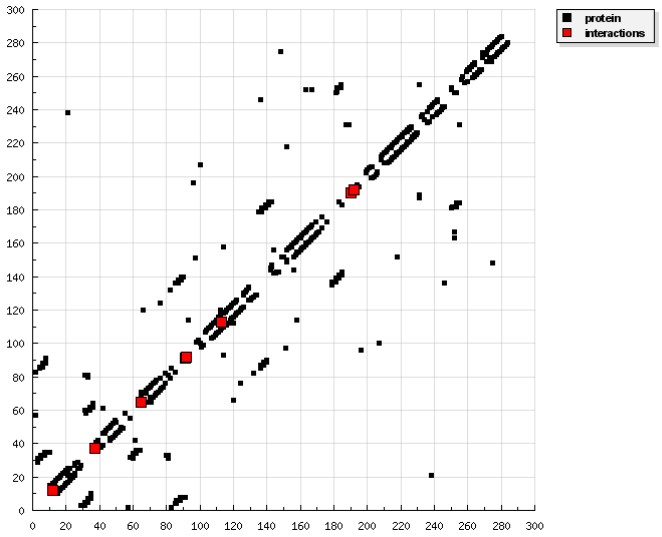

HL2

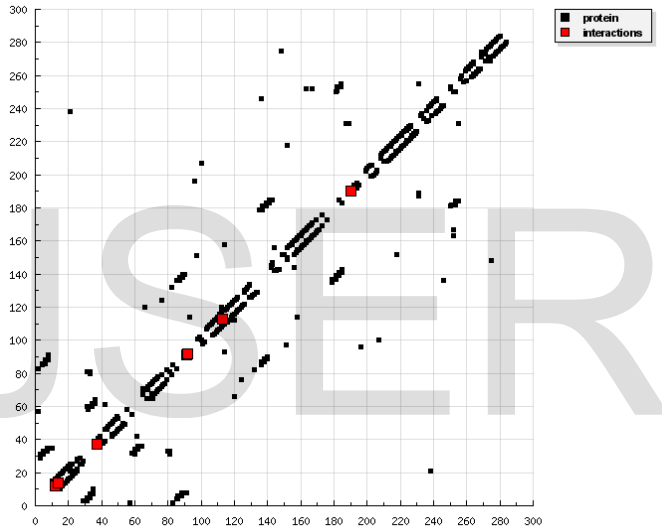

HL3

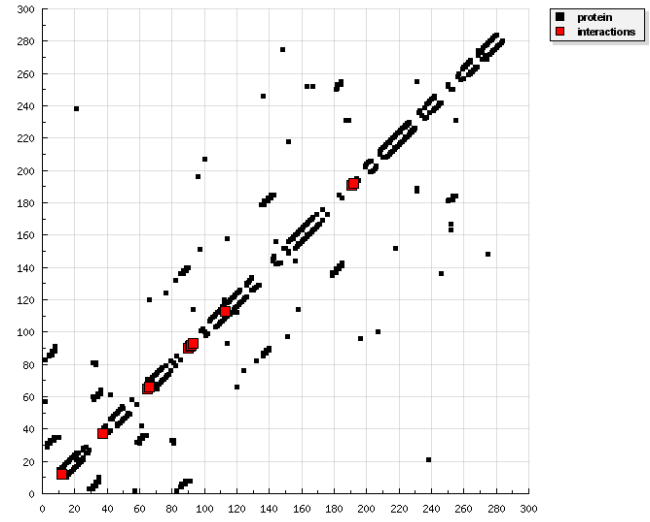

Fig. 8. HB plot of interaction between ligands (HL_n) with receptor of breast cancer mutant 3hb5.

HL1

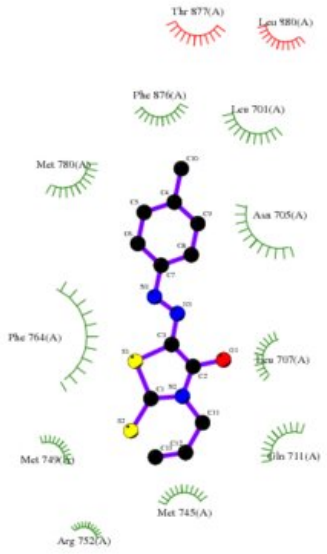

docking

HL2

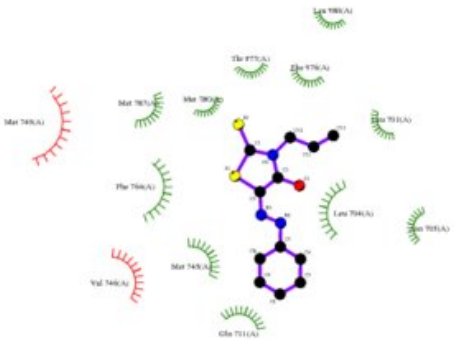

docking

HL3

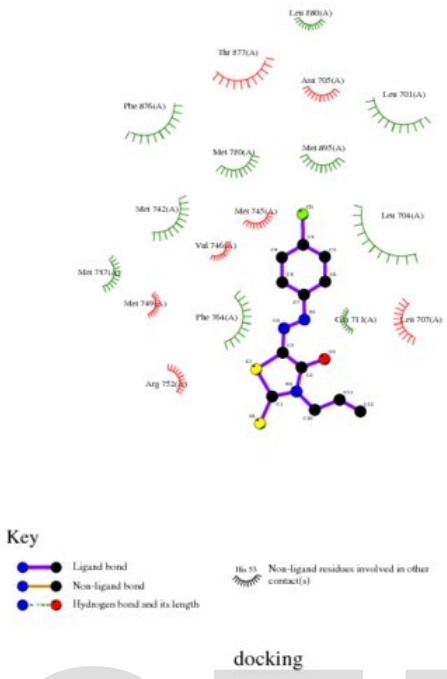

Fig. 9. 2D plot of interaction between ligands (HL_n) with receptor of prostate cancer mutant 2q7k.

HL1

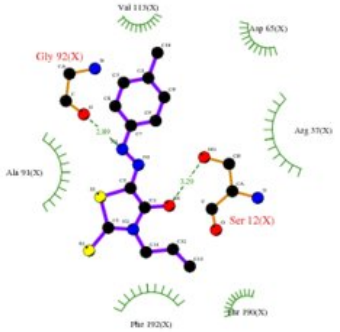

docking

HL2

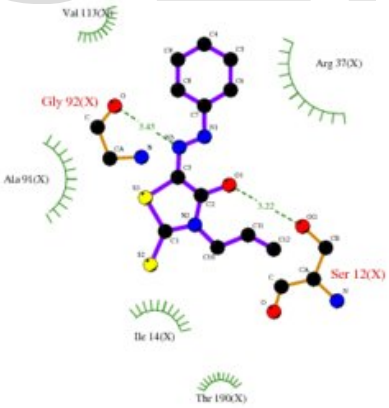

docking

HL3

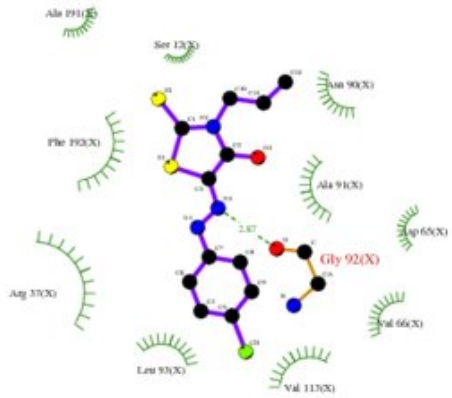

Fig. 10. 2D plot of interaction between ligands (HL_n) with receptor of breast cancer mutant 3hb5.

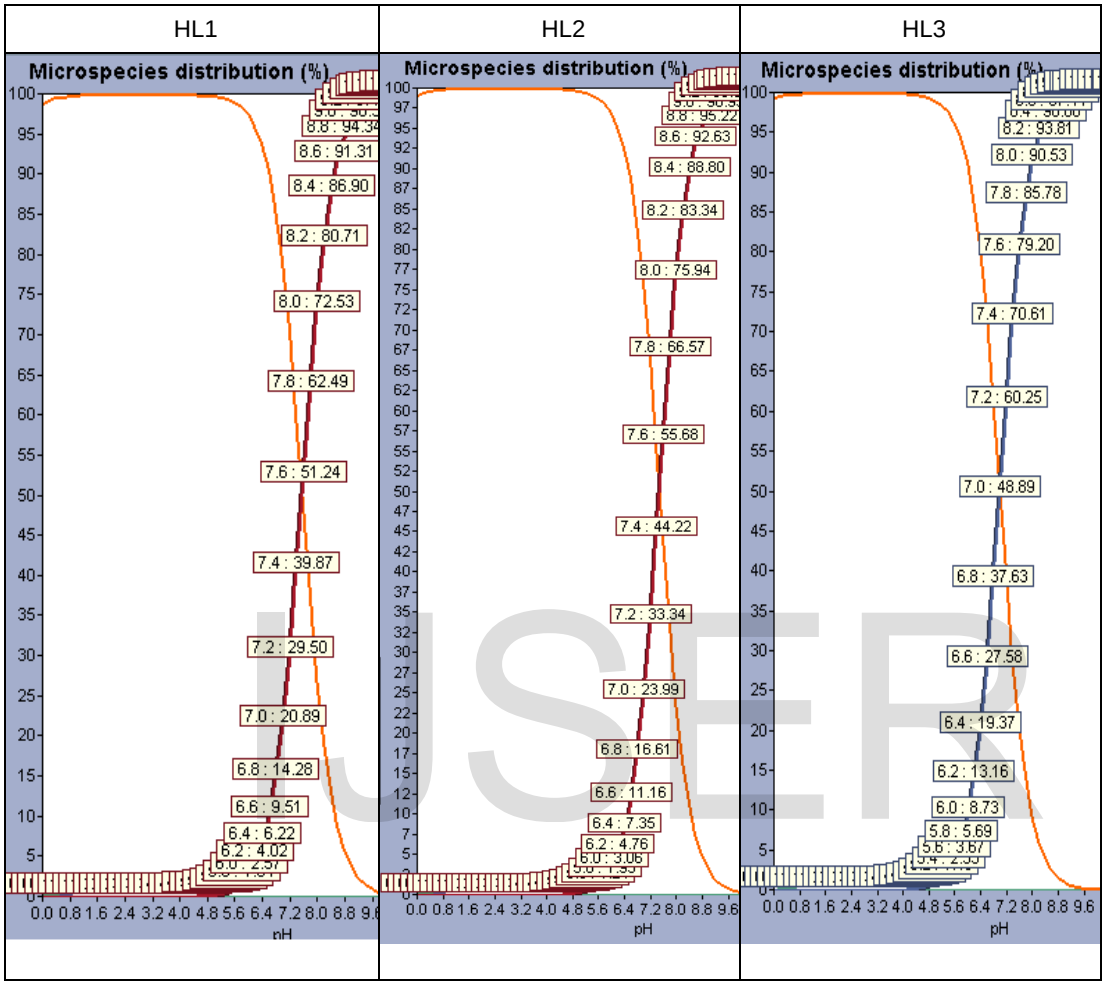

Fig. 11. Microspecies distribution curves of the ligands.

5. REFERENCES

[1] A.Z. El-Sonbati, M.A. Diab, M.M. El-Halawany, N.E. Salam, Mater. Chem. Phys. 123 (2010) 439–449.
[2] M.S. Azziz, A.Z. El-Sonbati, A.S. Hilali, Chem. Pap. 56 (2002) 305–308
[3] M.A. Elbagerma, G. Azimi, H.G.M. Edwards, A.I. Alatjtal, I.J. Scowen, Spectrochim. Acta A 75 (2010) 1403-1410.
[4] J. Lin, D.C. Sahakian, S.M.D. Morais, J.J. Xu, R.J. Polzer, Curr. Top. Med. Chem. 3 (2003) 1125-1154.
[5] N. Acar and T. Tulun, Eur, Polym. J. 37(2001) 1599-1605.
[6] A.A. El-Bindary, G.G.Mohamed, A.Z. El-Sonbati, M.A.Diab,W.M.I. Hassan, Sh.M. Morgan, A.K. Elkholy, J. Mol. Liq. 218 (2016) 138–149.
[7] A.F. Shoair, A.A. El-Bindary, A.Z. El-Sonbati, N.M. Beshry, J. Mol. Liq. 215 (2016) 740–748.
[8] A.A. El-Bindary, A.Z. El-Sonbati, M.A. Diab, E.E. El-Katori, H.A. Seyam, Int. J. Adv. Res. 2 (2014) 493-502.
[9] A.A. El-Bindary , A.F. Shoair, A.Z. El-Sonbati, M.A. Diab, E.E. Abdo, J. Mol. Liq. 212 (2015) 576–584.
[11] R.M. Issa, A.Z. El-Sonbati, A.A. El-Bindary, H. M. Kera, J. Inorg. Organom. Polym. 13 (2003) 269-283.
[12] A.Z. El-Sonbati, A.A. El-Bindary, N.A. El-Deeb, React. Funct. Polym. 50 (2002) 131-138.
[13] R.M. Issa, A.Z. El-Sonbati, A.A. El-Bindary, H. M. Kera, J. Eur. Polym 38 (2002) 561-566.
[14] A.A. El-Bindary, M.M. Ghoneim, M.A. Diab, A.Z. El-Sonbati, L.S. Serag, J Thermodyn Catal 5:135 (2014) (Doi:10.4172/2157-7544.1000135).
[15] A.Z. El-Sonbati, A.A.M. Belal, M.A. Diab, M.Z. Balboula, Spectrochim. Acta A 78 (2011) 1119–112.
[16] M.A. Diab, A.Z. El-Sonbati, A.A. El-Bindary, G.G. Mohamed, Sh.M. Morgan, Res. Chem. Intermed. 41 (2015) 9029–9066.
[17] A.Z. El-Sonbati, M.A. Diab, A.F. Shoair, A.A. El-Bindary, A.M. Barakat, J. Mol. Liq. 216 (2016) 821–829.
[18] A.A. El-Bindary, A.Z. El-Sonbati, M.A. Diab, Sh.M. Morgan, J. Mol. Liq. 201 (2015) 36–42.
[19] A.Z. El-Sonbati, A.A. El-Bindary, R.M. Ahmed, J. Sol. Chem. 32 (2003) 617–623.
[20] A.Z. El-Sonbati, M.A. Diab, A.A. El-Bindary, Sh.M. Morgan, Inorg. Chim. Acta 404 (2013) 175–187.
[21] A.A. Al-Sarawy, A.A. El-Bindary, A.Z. El-Sonbati, M.M. Mokpel, Polish J. Chem. 80 (2006) 289–295.
[22] A.Z. El-Sonbati, M.A. Diab, A.A. El-Bindary, A.M. Eldesoky, Sh.M. Morgan, Spectrochim. Acta A 135 (2015) 774–791.
[23] N.A. El-Ghamaz, A.Z. El-Sonbati, M.A. Diab, A.A. El-Bindary, G.G. Mohamed, Sh.M. Morgan, Spectrochim. Acta A 147 (2015) 200–211.
[24] N.A. El-Ghamaz, M.M. Ghoneim, A.Z. El-Sonbati, M.A. Diab, A.A. El-Bindary and M.K. Abd El-Kader, J. Saudi. Chem. Soc. (2014) DOI: 10.1016/j.jscs.2014.03.010.
[25] S.H. Lawrence, U.D. Ramirez, L. Tang, F. Fazliyez, L. Kundrat, G.D. Markham, E.K. Jaffe, Chem. Biol. 15 (2008) 586-596.
[26] Z. Bikadi, E. Hazai, J. Chem. Inf. 11 (2009) 1-15.
[27] T. A. Halgren, J. Computat. Chem. 17 (1998) 490-519.
[28] G.M. Morris, D.S. Goodsell, J. Comput. Chem. 19 (1998) 1639-1662.
[29] A.Z. El-Sonbati, M.A. Diab, M.S. El-Shehawy, M.M. Makpel, Spectrochim. Acta A 75 (2010) 394.
[30] A.Z. El-Sonbati, M.A. Diab, M.M. El-Halawany, N.E. Salam, Mater. Chem. Phys. 123 (2010) 439.
[31] A.M. Eldesoky, M.A. El-Bindary, A.Z. El-Sonbati, Sh.M. Morgan, J. Mater. Environ. Sci. 6 (2015) 2260-2276.
[32] K. Fukui, Orientation and Stereoselection, Vol. 15/1, Springer Berlin Heidelberg, 1970.
[33] A.Z. El-Sonbati, M.A. Diab, A.A. El-Bindary, G.G. Mohamed, Sh.M. Morgan, M.I. Abou-Dobara, S.G. Nozha, J. Mol. Liq. 215 (2016) 423–442.
[34] A.Z. El-Sonbati, M.A. Diab, A.A. El-Bindary and Sh.M. Morgan, Spectrochim. Acta A 127 (2014) 310-328.
[35] A. Beteringhe, C. Racuciu, C. Balan, E. Stoican, L. Patron, Adv. Mater. Res. 787 (2013) 236–240.
[36] N.M. Hosny, M.A. Hussien, F.M. Radwan, N. Nawar, Spectrochim. Acta A 132 (2014) 121–129.
[37] M.A. Diab, A.Z. El-Sonbati, A.A. El-Bindary, Sh.M. Morgan, M.K. Abd El-Kader, J. Mol. Liq. 218 (2016) 571–585.
[38] A.Z. El-Sonbati, M.A. Diab, A.A. El-Bindary, M.I. Abou-Dobara, H.A. Seyam, J. Mol. Liq. 218 (2016) 434–456.
[39] H. Irving, H.S. Rossotti. J. Chem. Soc., (1953) 3397.
[40] H. Irving, H.S. Rossotti. J. Chem. Soc., (1954) 2904.
[41] F.I.C. Rossotti, H.S. Rossotti. Acta Chem. Scand. 9 (1955) 1166.
[42] A.A.A. Boraei, N.F.A. Mohamed, J. Chem. Eng. Data 47 (2002) 987-991.
[43] P. Sanyal, G.P. Sengupta, Anil. J. Ind. Chem. Soc. 67 (1990) 342-346.
[44] S. Sridhar, P. Kulanthaipandi, P. Thillaiarasu, V. Thanikachalam, G. Manikandan, J. Chem. 4 (2009) 133-140.
[45] V.D. Athawale, V. Lele, J. Chem. Eng. Data 4 (1996). 1015-1019.
[46] V.D. Athawale, S.S. Nerkar, Monatsh Chem. 131 (2000) 267-276.
[47] F.A.A. Tirkistani, A.A. El-Bindary, Bull. Electrochem. 21 (2005) 265-269.
[48] G.A. Ibañez, G.M. Escandar, Polyhedron. 17 (1998) 4433-4441.
[49] W.U. Malik, G.D. Tuli, R.D. Madan, "Selected Topics in Inorganic Chemistry" , 3rd Ed., Chand S. and Company LTD, New Delhi, 1984.
[50] F.R. Harlly, R.M. Burgess, R.M. Alcock, "Solution Equilibria" , p. 257. Ellis Harwood, Chichester, 1980.
[51] L.E. Orgel "An introduction to transition metal chemistry ligand field theory" , p. 55. Methuen, London, 1966.
[52] A. Bebot-Bringaud, C. Dange, N. Fauconnier, C. Gerard, J. Inorg. Biochem. 75 (1999) 71-78.
[53] F.R. Harlly, R.M. Burgess, R.M. Alcock, "Solution Equilibria" , p. 257. Ellis Harwood, Chichester, 1980.
[54] M.T. Beck, I. Nagybal, Chemistry of Complex Equilibrium, Wiley, New York,1990.
[55] A.A. Al-Sarawy, A.A. El-Bindary, A.Z. El-Sonbati, T.Y. Omar, Chem. Pap. 59 (2005) 261-266.
[56] A.T. Mubarak, A.Z. El-Sonbati, A.A. El-Bindary, Chem. Pap. 58 (2004) 320-323.
[57] K.D. Bhesaniya, S. Baluja, J. Mol. Liq. 190 (2014) 190-195.